Historic, archived document

Do not assume content reflects current scientific knowledge, policies, or practices.

A99.9
F764U
cop.2

United States
Department of
Agriculture

Forest Service

**Intermountain
Forest and Range
Experiment Station**

Research Paper
INT-257

July 1982

Estimating Upslope Convective Windspeeds for Predicting Wildland Fire Behavior

F.A. Albini, D.J. Latham, and R.G. Baughman

THE AUTHORS

FRANK A. ALBINI is a mechanical engineer, assigned to the Fire Fundamentals research work unit at the Northern Forest Fire Laboratory in Missoula, Mont. He earned a Ph.D. from the California Institute of Technology in 1962, where he also obtained his undergraduate training (B.S. 1958, M.S. 1959). He joined the Forest Service in October 1973 after 12 years of pure and applied research and systems analysis both in private industry and at the nonprofit Institute for Defense Analyses.

DON J. LATHAM received his bachelor's degree in physics from Pomona College in 1960, his master's in 1964 and Ph.D. in 1967, both in Earth Science, from the New Mexico Institute of Mining and Technology. From 1968 to 1976 he taught and did research in atmospheric electricity in the Rosensteil School of Marine and Atmospheric Science, University of Miami. In 1976 he joined the Northern Forest Fire Laboratory as a research meteorologist/physicist.

ROBERT G. BAUGHMAN holds a B.S. and M.S. degree in meteorology and climatology from the University of Washington. From 1954 to 1958 he was engaged in arctic research with the U.S. Corps of Engineers. Since joining the Forest Service in 1958, he has held the position of research meteorologist at the Northern Forest Fire Laboratory and has been involved in research on thunderstorms, lightning, weather modification, and forest meteorology. Baughman retired from the Forest Service in December 1980.

RESEARCH SUMMARY

A mathematical model is developed that describes the convective flow of air up a sun-heated open slope under conditions of general calm. The model predicts quantitatively most of the features of the "slope wind" long recognized by practitioners of fire behavior and fire weather prediction. A limited first test of the model gave encouraging results. The model is applied to the calculation of midflame windspeeds for stylized fuel models used in current wildland fire behavior prediction techniques. Equations, graphs, and tabulated midflame windspeeds are presented. Further testing is needed to validate the predictions of the model; in the interim, the tables given here can be used as the best presently available data.

INTRODUCTION

Upslope winds are evidenced under otherwise calm conditions on open, sun-heated slopes. These local winds are the direct result of the heating of the air next to the slope. Although these winds are of modest force, their influence should be accounted for in wildland fire spread projections. The general features of the upslope convective windfield are well described by Schroeder and Buck (1970) as "slope winds":

> Slope winds are local diurnal winds present on all sloping surfaces. They flow upslope during the day as the result of surface heating, and downslope at night because of surface cooling. Slope winds are produced by the local pressure gradient caused by the difference in temperature between air near the slope and air at the same elevation away from the slope.
>
> During the daytime the warm air sheath next to the slope serves as a natural chimney and provides a path of least resistance for the upward flow of warm air···. Upslope winds are quite shallow but their depth increases from the lower portion of the slope to the upper portion···.

Although experienced firefighters and students of wildland fire behavior have long been aware of the upslope convective wind phenomenon, no theoretical or empirical model of the process has been available to permit quantitative estimates of expected windspeeds. The procedures available to the trained fire behavior officer in the form of field reference material[1] and pocket calculator programs (Burgan 1979) allow rapid prediction of wildland fire behavior once the necessary input data are assembled. In these procedures, the influence of wind on fire behavior is derived from the "midflame windspeed," or the average speed of the ambient windfield over the vertical extent of the flame. The field reference material contains aids for estimating surface speed and direction for general winds, and for calculating midflame windspeeds (Baughman and Albini 1980). This paper provides the equivalent procedure for the upslope convective wind.

Note that prediction of the upslope convective wind is not connected in any way to the prediction or description of the windfield associated with a fire. The "midflame windspeed" is an ambient windspeed used in fire behavior prediction. It enters into the rate-of-spread calculation as a parameter that empirically corrects rate of spread and other fire behavior calculations. The windfield in the near vicinity of, and especially further up the slope than, a fire on a slope will differ from that predicted by the model presented here. The fire behavior model of Rothermel (1972) implicitly accounts for the indraft wind induced by a fire on a slope, through the "slope factor" multiplying the rate of spread. We seek here only to characterize the additional influence of an ambient windfield that would exist in the absence of a fire, in the manner described by Albini and Baughman (1979).

A mathematical model for this windfield is derived in appendix A. The basic relationships included in the model express (1) a balance between the buoyancy force (the "pressure gradient" mentioned above) and the friction of the air flow along the surface, (2) a balance between the heat absorbed by the air from the warm slope and the carrying away of this heat by the motion of the air, and (3) a balance between the buoyancy force that acts to lift the air sheath off the slope and the action of turbulence produced by the air motion which acts to restrain it (the "natural chimney" mentioned above).

---

[1]National Wildfire Coordinating Group, 1979. Fire Behavior Officer's Field Reference, USDA For. Serv. Natl. Adv. Resource Technol. Cent., Marana Air Park, Ariz., looseleaf.

A more comprehensive model for slope winds, including both downslope ("drainage") and upslope ("convective") winds has been assembled by Ryan (1977) and incorporated into a broadly applicable simulation model. For predicting smoke transport and dispersal or simply to generate a map of surface winds in mountainous terrain, such a complex model is required. For the more limited application intended here, a simpler and more easily applied formulation was desired. Ryan's (1977) model gives explicit time-dependent predictions not only of windspeed but of direction, but the near-surface flow structure (i.e., the shear layer described in appendix A) is not specifically addressed.

The weakest assumption made in the course of developing the present model is that the surface of the slope has the same temperature at all elevations. If the source of heat is the sun's rays, this assumption can be defended by the argument that the temperature of the surface should be very nearly that which achieves a balance between the rate of solar heat absorption and the rate at which it is radiated away by the surface. This means that the amount of heat carried away by the air sheath and that conducted into the ground are both small compared to the incident solar heating and the re-radiated heat loss. This implied balance does not depend on elevation and is such a weak function of slope angle (for summer afternoons in midlatitudes) that the surface temperature of the valley floor should closely approximate the temperature of the slope surface. This fact is used in applying the model results to provide a very simple means of estimating midflame windspeeds.

WIND MODEL RESULTS

The idealized situation addressed by the mathematical model of appendix A is shown schematically in figure 1. This sketch shows a short segment of a sun-heated slope inclined at an angle α to the horizontal. The wind blows upslope, parallel to the inclined surface. The windspeed is zero at the surface, increasing to a maximum value of u_m at a distance ℓ_m from the surface, as shown.

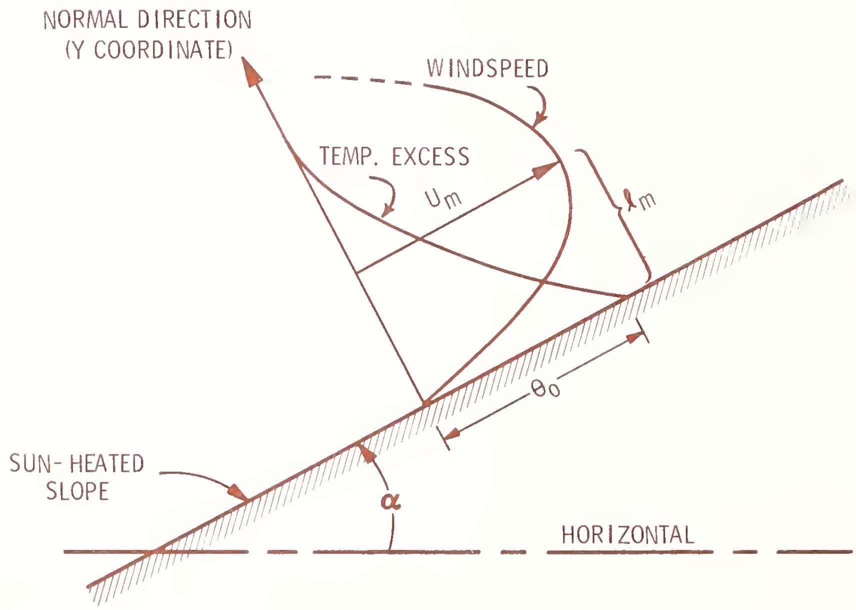

Figure 1.--Windspeed and temperature profiles in the near-surface layer of a sun-heated slope. Note that the y coordinate used to express model results is oriented perpendicular (or "normal") to the sloping surface. The windspeed reaches a maximum (u_m) at a distance ℓ_m from the surface, while the temperature excess falls from θ_o at the surface to zero at a distance of $2\ell_m$.

In the warm sheath of air over the surface, the temperature excess above the local ambient also varies with distance from the slope surface. The excess temperature is maximum at the surface and declines to zero at distance of $2\ell_m$ from the surface, as shown. Using the coordinate y to measure distance from the slope in the direction perpendicular to the slope, the variation of excess temperature (θ) and windspeed (u) with distance can be written as:

$$\theta = \theta_o \cos\left(\frac{\pi}{4}\, y/\ell_m\right) \exp\left(-\frac{\pi}{4}\, y/\ell_m\right) \quad (1)$$

$$u = u_m \sqrt{2}\, \sin\left(\frac{\pi}{4}\, y/\ell_m\right) \exp\left(\frac{\pi}{4}(1 - y/\ell_m)\right). \quad (2)$$

These profiles are accurately graphed in figure 2 up to the distance $y = \ell_m$. The variations expressed in equations (1) and (2) are thought to be accurate up to that distance but incorrect beyond the distance $y = 2\ell_m$. Between ℓ_m and $2\ell_m$ the values are probably accurate enough for present purposes.

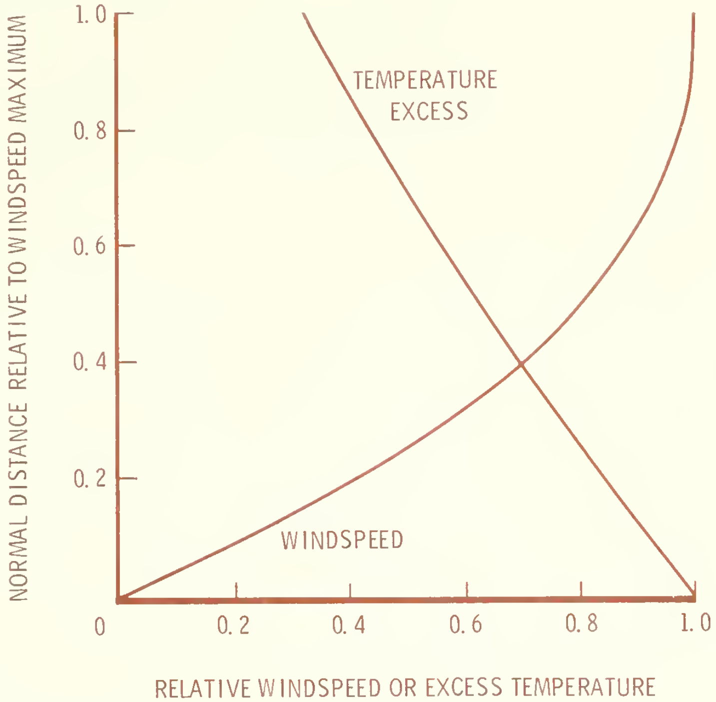

Figure 2.--Profiles of temperature excess and windspeed on a sun-heated slope, as predicted by the mathematical model of appendix A.

The windspeed and excess temperature maxima are, of course, related. The higher the excess temperature, the greater the buoyant force to be countered by friction, so the greater the windspeed. This model fixes the relationship as linear:

$$u_m = \exp(-\pi/4)\,(C_p/2T_a)^{1/2}\,\theta_o \quad (3)$$

where

C_p is the specific heat capacity of air at constant pressure = $1005\ m^2 s^{-2} {}^\circ K^{-1} = 6010\ ft^2 s^{-2} {}^\circ R^{-1}$

T_a is the absolute temperature (°K or °R) of the atmosphere, free of the slope influence, at the elevation in question.

If the ambient temperature is taken to be 32°C (90°F) or, in absolute degrees 305°K (549°R), then

$$u_m \doteq \begin{cases} 0.6\ \theta_o & \text{m/s}, \quad \theta_o \text{ in °C} \\ 1.1\ \theta_o & \text{ft/s}, \quad \theta_o \text{ in °F}. \end{cases} \tag{4}$$

The normal distance from the surface of the slope to the maximum windspeed, ℓ_m, is related to the maximum windspeed by an internal consistency requirement outlined in appendix A. The relationship that results from this argument is again linear and involves the angle of the slope:

$$\ell_m = 0.0158(C_p T_a)^{1/2} u_m/g \sin \alpha \tag{5}$$

where g is the acceleration of gravity = 9.81 m/s^2 (32.2 ft/s^2). Using the same ambient temperature as before, this can be expressed simply as the ratio of ℓ_m and u_m measured in seconds:

$$\ell_m/u_m = 0.892/\sin \alpha, \quad s. \tag{6}$$

This equation is graphed in figure 3. It is necessary to make use of this relationship to estimate midflame windspeed for some types of fuels.

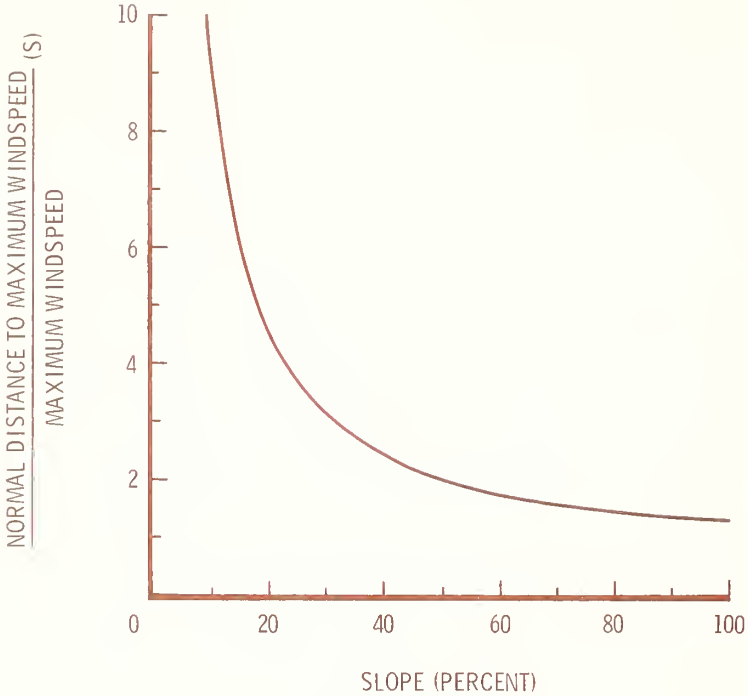

Figure 3.--Ratio of the normal distance of the maximum windspeed to the maximum windspeed, expressed in seconds.

The model results give quantitative expressions for the qualitative descriptions of the flow features quoted above from Schroeder and Buck (1970). Equation (4) expresses the relationship between the temperature excess on the surface of the slope and the maximum upslope windspeed.[2] The hotter the slope, relative to the temperature of the atmosphere

---

[2]Equation 4 also implies the direction of the wind. If slope surface cools, the implication of (4) is that the wind blows downslope, as it should. Nevertheless, the model should not be used for downslope winds because important physical factors have not been accounted for.

at the same elevation, the greater the induced windspeed. Because the temperature of the atmosphere on summer afternoons decreases with height, and the slope-surface temperature is assumed to be constant, the *excess* temperature on the slope surface increases with elevation above the valley floor. This implies greater windspeeds higher up the slope.

The excess temperature on the slope surface, θ_o, is determined by establishing the air temperature at the surface and subtracting the temperature of the free atmosphere at the elevation in question. On calm, sunny days, the temperature lapse rate of the air immediately above the ground exceeds the dry adiabatic rate. Data given by Sutton (1953) and Geiger (1966) indicate that this overwarm layer is about 100 m deep above a flat, grass-covered surface. The temperature at the surface is 4-5°C above the extrapolated dry adiabatic level. This value is supported by data from Lettau and Davidson (1957) that show temperature differences of about 5°C between 0.1 m and 16 m above mown grass on sunny afternoons.

Probably no exact value can be found to represent the temperature difference between the surface air and the air at the height where the dry adiabatic lapse rate begins during the hottest part of sunny days, but based on the above we shall use 5°C for our purposes. So θ_o can be approximated as 5°C plus the drop in temperature to the elevation of the point on the slope for which θ_o is being estimated. That is:

$$\theta_o \doteq \begin{cases} 5.0 + 0.01z, & \text{°C (z in m)} \\ 9.0 + 0.0055z, & \text{°F (z in ft)} \end{cases} \qquad (7)$$

where z is elevation above the valley floor. This simple form, used with (4), gives the maximum upslope convective windspeed as:

$$u_m \doteq \begin{cases} 3.0 + 0.006z, & \text{m/s (z in m)} \\ 9.9 + 0.006z, & \text{ft/s (z in ft).} \end{cases} \qquad (8)$$

This equation is graphed in figure 4.

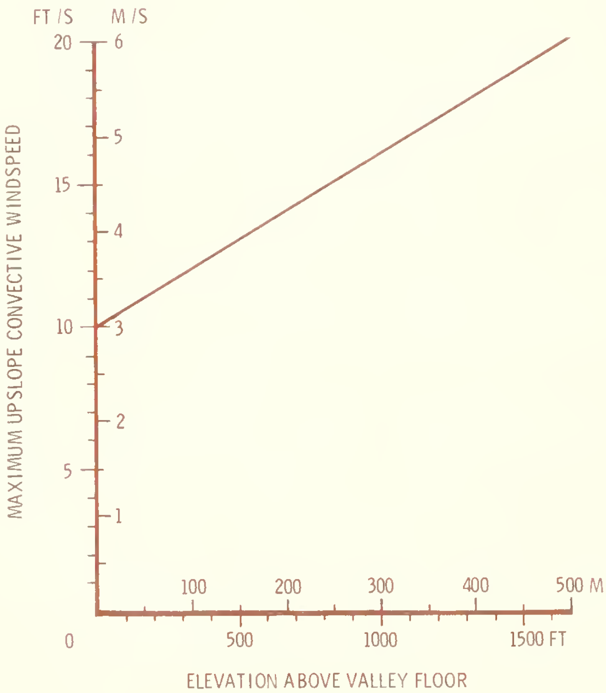

Figure 4.--Maximum upslope convective windspeed versus elevation above valley floor.

The "depth" of the slope wind layer can be taken as ℓ_m. Equation (6) indicates that this depth grows linearly with u_m and hence increases with distance up the slope. It also indicates that the depth decreases as the slope gets steeper, an intuitively appealing dependence.

Measurements in the field are often made at distances from the slope, y, which are small compared to ℓ_m, the depth of the wind layer. In this case, the general equation (2) for variation of windspeed with perpendicular distance from the slope reduces to:

$$u \doteq (\pi/2\sqrt{2})\exp(\pi/4)u_m(y/\ell_m), \quad y<<\ell_m. \tag{9}$$

Now put in u_m/ℓ_m from equation (6), and:

$$u/y \doteq 2.74 \sin \alpha, \quad s^{-1}. \tag{10}$$

This means that if the distance from the slope is small compared to the distance to the maximum windspeed, the measured windspeed is independent of the elevation of the measuring point above the valley floor.

One can use a relationship much like (10) in applying the model results to fire behavior prediction for quickly estimating midflame windspeed. A "global" approximation of the lower part of the profile is:

$$u/u_m \doteq 2y/\ell_m. \tag{11}$$

Equation (11) underpredicts the windspeed slightly for y/ℓ_m less than 0.25 and overpredicts slightly for y/ℓ_m greater than 0.25. But over the whole range from 0 to 0.4, it is a good approximation, as can be verified by overlaying a straightedge on figure 2.

TEST OF THE MODEL

Windspeed, temperature, and humidity were continuously monitored for about one year on the site of an experimental prescribed burn area near the Northern Forest Fire Laboratory. These data afforded the opportunity to test the model developed here. The site was a small valley on the east fork of O'Keefe Creek, about 10 miles northwest of Missoula, Mont.

The valley is about 4.8 km (3 mi) long and 1.6 km (1 mi) wide. Windspeed measurements were taken at an elevation 140 m (460 ft) above the creek on a south-facing 22 percent slope, covered by a mixture of grass, shrubs, and an open stand of ponderosa pine. The anemometer was located about 6.1 m (20 ft) above a grassy portion of the slope, about 90 m (300 ft) upslope of the nearest trees.

Recordings were made by a 3-cup anemometer that made an electrical contact, causing a mark on a paper chart for each 5 miles of air passage (i.e., each 5 mile wind run). The contacts were recorded on a hygrothermograph chart, which provided a time reference.

Review of the synoptic charts and daily readings from the local National Weather Service station (located at the Missoula airport, about 4 miles from the observation site) revealed that there were five sunny days during the recording period of 1979 on which the general winds were light enough to allow measurement of the upslope convective windspeed.

Because maximum winds and heating were desired for the days in question, wind-run charts were examined for maxima during the afternoon hours (1400-1800 LDT). The maximum velocity for a 10 mile run, i.e., two successive 5 mile runs, was taken as data for model verification. These data are given in the following tabulation:

Date (1979)	Recorded maximum windspeed, mi/h
7/24	4.2
8/2	5.7
8/4	5.5
8/7	5.7
9/7	5.7
Average	5.36 mi/h (2.39 m/s)
Standard deviation	0.65 mi/h (0.29 m/s)

The model predicts a maximum upslope windspeed of 3.85 m/s (fig. 4) at a normal distance from the slope of 16.2 m (fig. 3). At[3] the instrument height of 6.1 m, or 0.35 of the normal distance to the maximum windspeed, figure 2 indicates a sensed windspeed of 0.64 times the maximum, or 2.46 m/s (5.51 mi/h).

The degree of agreement between the predicted and observed windspeeds is gratifying, but obviously not a rigorous test of the model. The near-constancy of the maximum recorded windspeeds on different days is likewise not conclusive but is encouraging.

APPLICATION TO FIRE BEHAVIOR PREDICTION

Midflame windspeeds can be calculated using the model presented here, once the geometry of the fuelbed and the flame above it are established. Using the assumptions and mathematical manipulations outlined in appendix B, tables of midflame windspeeds were developed for the 10 stylized fuel models that might be used for predicting fire behavior on open slopes. Fuel models 7, 8, and 9 were not included because they are used only for fuels under standing timber (Albini 1976). Model 10, also an understory fuel model, is sometimes used to represent logging slash overgrown with shrubs, grasses, and forbs, so was included. Tree cover on the slope both interferes with the solar heating of the surface and obstructs the development of the convective windfield, therefore the model cannot be used for tree-covered slopes.

Two cases were considered:

1. The slope is uniformly covered with the fuel model below the fire site, and

2. The slope below the fire site is free of cover.

The first situation might represent a prescribed burn, an ignition on the slope, or a fire backing down the slope. The second situation might represent a slope with a rock or scree face, or a fire burning upslope from near the base.

---

[3]Both instrument height and distance to the maximum windspeed should be adjusted for displacement of the zero-windspeed surface (appendix B), but the unknown cover height prevents this step. Doing so would raise the predicted windspeed slightly.

The fuel models used can be divided into "shallow" and "deep" fuelbeds. The "shallow" fuelbeds, represented by models 1, 2, 5, 6, 10, and 11, have fuelbed depths and typical flame heights small enough that the variation of windspeed with distance from the slope given in equation 10 is a good approximation in all cases. Midflame windspeeds for these models are thus a function of slope only. Table 1 gives midflame windspeeds for these models.

The "deep" fuelbeds, represented by stylized models 3, 4, 12, and 13, exhibit some degree of dependence of midflame windspeed on both slope and elevation above the valley floor, because the fuelbed depths and flame heights exceed the linear windspeed-vs.-distance regime for which equation 10 applies. Table 2 gives the midflame windspeeds for these models for the case of uniform cover below the fire site. For the case of a bare slope below the fire site, use table 3.

Table 1. Midflame windspeeds (mi/h) for "shallow" fuelbeds with upslope convection winds

Fuel model	Slope percent								
	20	30	40	50	60	70	80	90	100
Slope below fire site uniformly vegetated									
1. Short grass	0.3	0.4	0.5	0.6	0.7	0.8	0.8	0.9	0.9
2. Open timber (grass and understory)	.4	.5	.7	.8	.9	1.0	1.1	1.2	1.3
5. Brush	.3	.5	.6	.7	.8	.9	1.0	1.1	1.2
6. Dormant brush, hardwood slash	.5	.7	.9	1.0	1.2	1.3	1.4	1.5	1.6
10. Overgrown slash	.4	.5	.7	.8	.9	1.0	1.1	1.2	1.3
11. Light conifer slash	.3	.4	.5	.6	.7	.8	.9	.9	1.0
Slope below fire site free of vegetation									
1. Short grass	0.5	0.8	1.0	1.2	1.4	1.5	1.6	1.8	1.9
2. Open timber (grass and understory)	.6	.9	1.2	1.4	1.6	1.8	1.9	2.1	2.2
5. Brush	.9	1.3	1.6	1.9	2.2	2.4	2.6	2.8	2.9
6. Dormant brush, hardwood slash	1.1	1.6	2.1	2.5	2.8	3.1	3.3	3.5	3.7
10. Overgrown slash	.6	.9	1.2	1.4	1.6	1.8	1.9	2.1	2.2
11. Light conifer slash	.6	.8	1.0	1.2	1.4	1.6	1.7	1.8	1.9

Table 2. Midflame windspeeds (mi/h) for "deep" fuelbed models with upslope convection winds. Slope uniformly covered with vegetation below fire site

Fuel model	Elevation, feet (above valley floor)	Slope, percent								
		20	30	40	50	60	70	80	90	100
Model 3	0-300	0.7	1.0	1.2	1.5	1.7	1.9	2.0	2.1	2.2
Tall grass	300-600	.7	1.0	1.3	1.5	1.7	1.9	2.0	2.2	2.3
	600-900	.7	1.0	1.3	1.5	1.7	1.9	2.1	2.2	2.3
	900-1200	.7	1.0	1.3	1.5	1.7	1.9	2.1	2.2	2.3
	1200-1500	.7	1.0	1.3	1.5	1.7	1.9	2.1	2.2	2.3
Model 4	0-300	1.3	1.9	2.3	2.7	3.0	3.3	3.5	3.7	3.9
Chaparral	300-600	1.3	1.9	2.4	2.8	3.1	3.4	3.7	3.9	4.0
	600-900	1.3	1.9	2.4	2.8	3.2	3.5	3.8	4.0	4.2
	900-1200	1.3	1.9	2.4	2.9	3.2	3.6	3.8	4.1	4.3
	1200-1500	1.3	1.9	2.4	2.9	3.3	3.6	3.9	4.1	4.3
Model 12	0-300	.7	1.0	1.2	1.4	1.6	1.8	2.0	2.1	2.2
Medium conifer	300-600	.7	1.0	1.2	1.5	1.7	1.8	2.0	2.1	2.2
slash	600-900	.7	1.0	1.2	1.5	1.7	1.9	2.0	2.1	2.3
	900-1200	.7	1.0	1.2	1.5	1.7	1.9	2.0	2.2	2.3
	1200-1500	.7	1.0	1.3	1.5	1.7	1.9	2.0	2.2	2.3
Model 13	0-300	.9	1.3	1.6	1.9	2.1	2.4	2.5	2.7	2.8
Heavy conifer	300-600	.9	1.3	1.6	1.9	2.2	2.4	2.6	2.7	2.9
slash	600-900	.9	1.3	1.6	2.0	2.2	2.4	2.6	2.8	2.9
	900-1200	.9	1.3	1.7	2.0	2.2	2.5	2.7	2.8	3.0
	1200-1500	.9	1.3	1.7	2.0	2.3	2.5	2.7	2.9	3.0

Table 3. Midflame windspeeds (mi/h) for "deep" fuelbed models with upslope convection winds. Slope bare of vegetation below fire site

Fuel model	Elevation, feet (above valley floor)	Slope, percent								
		20	30	40	50	60	70	80	90	100
Model 3	0-300	1.3	1.9	2.4	2.8	3.1	3.4	3.6	3.8	4.0
Tall grass	300-600	1.3	1.9	2.4	2.8	3.2	3.5	3.7	4.0	4.1
	600-900	1.3	1.9	2.4	2.9	3.2	3.6	3.8	4.1	4.2
	900-1200	1.4	1.9	2.5	2.9	3.3	3.6	3.9	4.1	4.3
	1200-1500	1.4	2.0	2.5	2.9	3.3	3.7	4.0	4.2	4.4
Model 4	0-300	2.7	3.7	4.4	5.0	5.5	5.8	6.1	6.3	6.5
Chaparral	300-600	2.7	3.8	4.6	5.3	5.8	6.2	6.6	6.8	7.0
	600-900	2.8	3.9	4.8	5.5	6.1	6.5	6.9	7.2	7.5
	900-1200	2.8	3.9	4.9	5.7	6.3	6.8	7.2	7.5	7.8
	1200-1500	2.8	4.0	5.0	5.8	6.5	7.0	7.4	7.8	8.1
Model 12	0-300	1.3	1.8	2.2	2.6	3.0	3.2	3.5	3.7	3.8
Medium conifer	300-600	1.3	1.8	2.3	2.7	3.0	3.3	3.6	3.8	4.0
slash	600-900	1.3	1.8	2.3	2.7	3.1	3.4	3.7	3.9	4.1
	900-1200	1.3	1.8	2.3	2.8	3.1	3.5	3.7	3.9	4.1
	1200-1500	1.3	1.9	2.4	2.8	3.2	3.5	3.8	4.0	4.2
Model 13	0-300	1.6	2.3	2.9	3.3	3.7	4.0	4.3	4.5	4.7
Heavy conifer	300-600	1.7	2.3	2.9	3.4	3.8	4.2	4.5	4.7	4.9
slash	600-900	1.7	2.4	3.0	3.5	3.9	4.3	4.6	4.9	5.1
	900-1200	1.7	2.4	3.0	3.6	4.0	4.4	4.7	5.0	5.2
	1200-1500	1.7	2.4	3.1	3.6	4.1	4.5	4.8	5.1	5.3

PUBLICATIONS CITED

Albini, F. A., and R. G. Baughman.
1979. Estimating windspeeds for predicting wildland fire behavior. USDA For. Serv. Res. Pap. INT-221, 12 p. Intermt. For. and Range Exp. Stn., Ogden, Utah.

Albini, Frank A.
1976. Estimating wildfire behavior and effects. USDA For. Serv. Gen. Tech. Rep. INT-30, 92 p. Intermt. For. and Range Exp. Stn., Ogden, Utah.

Baughman, R. G., and F. A. Albini.
1980. Estimating midflame windspeeds. *In* Proc. sixth conf. on fire and for. meteorol. p. 88-92. Robert E. Martin and others, eds. Soc. Amer. For., Washington, D.C.

Burgan, Robert E.
1979. Fire danger/fire behavior computations with the Texas Instruments TI-59 calculator: user's manual. USDA For. Serv. Gen. Tech. Rep. INT-61, 25 p. Intermt. For. and Range Exp. Stn., Ogden, Utah.

Defant, Friedrick.
1951. Local winds. *In* Compendium of meteorology. p. 655-672. Thomas F. Malone, ed. Amer. Meteorol. Soc., Boston, Mass.

Geiger, Rudolf.
1966. The climate near the ground. Transl. by Scripta Technica, Inc., of 4th German ed. 611 p. Harvard Univ. Press, Cambridge, Mass.

Lettau, Heinz H., and Ben Davidson, eds.
1957. Exploring the atmosphere's first mile, vol. II. 578 p. Pergamon Press, London.

Prandtl, L.
1952. Essentials of fluid dynamics. 431 p. Hafner Publishing Co., New York.

Rothermel, Richard C.
1972. A mathematical model for predicting fire spread in wildland fuels. USDA For. Serv. Res. Pap. INT-115, 40 p. Intermt. For. and Range Exp. Stn., Ogden, Utah.

Ryan, B. C.
1977. A mathematical model for diagnosis and prediction of surface winds in mountainous terrain. J. Appl. Meteorol. 16:571-584.

Schroeder, Mark J., and Charles C. Buck.
1970. Fire weather: a guide for application of meteorological information to forest fire control applications. USDA For. Serv., Agric. Handbook 360, 229 p. U.S. Govt. Printing Off., Washington, D.C.

Sutton, O. G.
1953. Micrometeorology. 333 p. McGraw-Hill Book Co., New York.

Tennekes, H., and J. L. Lumley.
1972. A first course in turbulence. 300 p. MIT Press, Cambridge, Mass.

APPENDIX A: CONVECTIVE SLOPE WIND MODEL

The equations describing steady two-dimensional turbulent flow of a compressible fluid under the combined influences of heat transport and gravity-induced body force can be written as:

$$\frac{\partial}{\partial x}(\rho u) + \frac{\partial}{\partial y}(\rho v) = 0 \tag{1}$$

$$\frac{\partial}{\partial x}(\rho u^2) + \frac{\partial}{\partial y}(\rho uv) = -\frac{\partial p}{\partial x} + \frac{\partial}{\partial x}\tau_{xx} + \frac{\partial}{\partial y}\tau_{xy} + \rho g_x \tag{2}$$

$$\frac{\partial}{\partial x}(\rho uv) + \frac{\partial}{\partial y}(\rho v^2) = -\frac{\partial p}{\partial y} + \frac{\partial}{\partial x}\tau_{xy} + \frac{\partial}{\partial y}\tau_{yy} + \rho g_y \tag{3}$$

$$\frac{\partial}{\partial x}(\rho uJ) + \frac{\partial}{\partial y}(\rho vJ) = \frac{\partial}{\partial x}(u\tau_{xx} + v\tau_{xy}) + \frac{\partial}{\partial y}(u\tau_{xy} + v\tau_{yy}) - \frac{\partial}{\partial x}q_x - \frac{\partial}{\partial y}q_y + \rho(ug_x + vg_y) \tag{4}$$

where

x is the direction along the slope, positive upward

y is normal to the slope, positive upward

ρ is the mean fluid density

(u,v) is the mean fluid velocity vector

p is the mean static pressure

τ_{ij} is the mean turbulent stress in the i plane, direction j

(g_x,g_y) is the gravity acceleration vector

J is the mean total enthalpy of the fluid

(q_x,q_y) is the heat flux vector.

Here we have neglected viscosity and correlations of fluctuations in the velocity field with density and pressure fluctuations, and used the fact that $\tau_{ij} = \tau_{ji}$.

Assuming that air is a perfect gas, we have:

$$J = C_p T + (u^2 + v^2)/2 \tag{5}$$

where T is the absolute temperature of the gas and C_p is its specific heat capacity at constant pressure. Multiplying the momentum equations (2) by u and (3) by v and summing gives the equation for the kinetic energy contribution to J. Subtracting this result from the energy equation yields the equation for the transport of sensible heat:

$$\rho C_p\left(u\frac{\partial T}{\partial x} + v\frac{\partial T}{\partial y}\right) = u\frac{\partial p}{\partial x} + v\frac{\partial p}{\partial y} - \frac{\partial}{\partial x}q_x - \frac{\partial}{\partial y}q_y + \{KE\}. \tag{6}$$

The term

$$\{KE\} = \tau_{xx}\frac{\partial u}{\partial x} + \tau_{yy}\frac{\partial v}{\partial y} + \tau_{xy}\left(\frac{\partial u}{\partial y} + \frac{\partial v}{\partial x}\right) \tag{7}$$

represents the generation of sensible heat through dissipation of kinetic energy by turbulent stress-strain work. This term can be neglected because the Mach number of the flow is very small; it has a magnitude relative to the others of the order of the square of the Mach number.

We now introduce the additional assumptions and approximations that describe the problem at hand:

1. The static pressure field is imposed by the ambient (quiescent) atmosphere and is not modified by the velocity field of the fluid flowing near the surface of the slope.

2. The mean velocity normal to the slope (v) vanishes everywhere.

This approximation implies that the boundary-layer flow along the surface of the slope evolves very slowly with distance (x) along the slope compared to the variations in the velocity and temperature fields normal to and near the surface of the slope. It also requires that the pressure gradient and body force terms of the normal momentum equation (3) be balanced by the turbulent normal stress gradient $(\frac{\partial}{\partial y}\tau_{yy})$. This implies a substantial variation with distance normal to the slope (y) of the normal turbulence intensity but the maximum value needed to satisfy (3) can be shown to be quite modest.

3. We neglect any variation with distance (x) along the slope of the temperature and velocity in comparison with their variations with distance normal to the slope (y).

Invoking these approximations and their immediate implications reduces the equation set dramatically. The sensible heat equation becomes

$$u\,\frac{\partial p}{\partial x} = -\rho_a g(\sin\alpha)u = \frac{\partial}{\partial y}q_y \tag{8}$$

and the momentum equation parallel to the slope

$$\frac{\partial p}{\partial x} - \rho g_x = -\rho_a g\sin\alpha + \rho g\sin\alpha = \frac{\partial}{\partial y}\tau_{xy} \tag{9}$$

where ρ_a represents the density of the ambient atmosphere and α is the slope angle from horizontal. For a perfect gas

$$p = \rho RT \tag{10}$$

where R is the gas constant; hence

$$\frac{\partial}{\partial y}\tau_{xy} = -\rho_a g\sin\alpha\left(\frac{T - T_a}{T}\right). \tag{11}$$

T_a is the temperature of the ambient atmosphere (a weak function of elevation).

The model is completed by specifying phenomenological forms for the turbulent transport of sensible heat and momentum. We follow the example of Defant (1951) and posit the forms:

$$\frac{1}{\rho}\frac{\partial}{\partial y}\tau_{xy} = K_m \frac{\partial^2 u}{\partial y^2} \tag{12}$$

$$\frac{1}{\rho_a C_p}\frac{\partial}{\partial y}q_y = -K_h \frac{\partial^2 T}{\partial y^2} . \tag{13}$$

The phenomenological factors K_m and K_h have the dimensions of length^2/time and are usually termed "eddy diffusivities" (Tennekes and Lumley 1972). They are almost always treated as constants for mathematical manipulations but are invariably found to be relatively strong functions of local conditions when measurement data are manipulated to determine their numerical values. But physical reasoning and dimensional arguments support the supposition that they are approximately equal no matter what their values. Usually the modeler treats these parameters as constants of flow structure (not fluid properties) and determines appropriate numerical values for them after the fact by matching observed and predicted features of the flow field or by invoking arguments for internal model consistency. We shall follow the latter course in this development and also assume at the outset that

$$K_m = K_h = K. \tag{14}$$

We shall treat the parameter K as a constant in developing the model. Then, using the shear stress (τ_{xy}) distribution predicted by the model, we apply a well accepted formula to calculate the local value of the parameter K. We average this expression over the important part of the boundary layer and so find a self-consistent average value to use for the parameter K.

Expressing the temperature in the boundary layer over the heated slope as the excess (θ) above the local ambient temperature

$$T = T_a + \theta \tag{15}$$

and using (12) in (11) and (13) in (8) gives the final form of the model:

$$K \frac{\partial^2 u}{\partial y^2} = - \frac{g \sin \alpha}{T_a} \theta \tag{16}$$

$$K \frac{\partial^2 \theta}{\partial y^2} = \frac{g \sin \alpha}{C_p} u \tag{17}$$

A remarkable feature of this model is that the equations (16) and (17) are formally identical to those of Defant (1951) who treated the similar problem of valley ventilation by upslope convection during early daytime heating. The mechanisms at play in these two instances are subtly but importantly different. Note, for instance, that in the development of this model, the temperature lapse rate of the ambient atmosphere does not explicitly enter. In Defant's development, the group g/C_p (which is the dry adiabatic lapse rate) in (17) is replaced by the lapse rate of the *potential* temperature in the ambient atmosphere, which measurement has determined usually to be zero for summertime afternoon conditions under which the upslope convective wind is generally the strongest (Schroeder and Buck 1970), but which is often positive over valleys in the morning when the surface temperature is lowest. So while the formalism of Defant's model applies directly here, the parameter groups are quite different and Defant's length scale is much greater than that found here. Indeed Defant's solution and the present one are formally identical to the rigorous solution of this problem for laminar flow found by L. Prandtl much earlier (to be found in translation in Prandtl 1952).

Differentiating (16) twice and using (17) gives

$$\frac{d^4u}{dy^4} + \left(\frac{g \sin \alpha}{K}\right)^2 \frac{u}{C_pT_a} = 0 \tag{18}$$

which establishes a characteristic length scale, ℓ, for the problem as

$$\ell = \left(\frac{4K^2C_pT_a}{(g \sin \alpha)^2}\right)^{1/4} \tag{19}$$

where the numerical factor 4 is introduced for convenience in writing the solution to (18). In terms of the dimensionless normal distance from the surface of the slope

$$\zeta = y/\ell \tag{20}$$

(18) becomes

$$\frac{d^4u}{d\zeta^4} + 4u = 0. \tag{21}$$

This equation has the general solution

$$u = (A \sin \zeta + B \cos \zeta)\exp(\zeta) + (C \sin \zeta + D \cos \zeta)\exp(-\zeta). \tag{22}$$

The positive exponential solutions are dismissed as nonphysical and the boundary condition

$$u(0) = 0 \tag{23}$$

requires D to be zero, leaving

$$u = C(\sin \zeta)\exp(-\zeta). \tag{24}$$

In terms of the temperature excess at the surface of the slope, θ_o, and the maximum windspeed, u_m, which occurs at $\zeta = \pi/4$, these profiles are

$$\theta = \theta_o(\cos \zeta)\exp(-\zeta) \tag{26}$$

$$u = u_m(\sin \zeta)\exp(-\zeta) \sqrt{2} \exp(\pi/4). \tag{27}$$

The profiles are graphed in the text, figure 2.

The validity of the profile of windspeed beyond the point at which it reaches maximum is questionable, and it is definitely not to be extended beyond $\zeta = \pi/2$ where the model predicts that the temperature falls below ambient. Near the surface, however, the profiles are quite reasonable, the velocity increasing linearly with distance normal to the surface and the temperature linearly declining. In fact, the windspeed profile can be well approximated up to about $0.4\ell_m$ (where $\ell_m = (\pi/4)\ell$ is the distance, along the normal to the slope, to the maximum windspeed) by the form

$$u \doteq 2u_m y/\ell_m \qquad (y \leq 0.4\ell_m). \tag{28}$$

In this linear profile regime, the turbulent shear stress predicted by this model (eq. 12) is constant at a value of

$$\tau_{xy} = \rho_a K \frac{\partial u}{\partial y} = 2\rho_a u_m K/\ell_m = \rho_a u_*^2. \qquad (29)$$

Above this constant-stress zone, the shear stress declines rapidly and is zero at the height (ℓ_m) of the maximum windspeed. Many measurements have been made of atmospheric shear layers to determine the structure of the turbulence fields. A general finding of such measurements is that the apparent eddy diffusivity, K, is proportional to the distance from the surface for constant shear layers (Tennekes and Lumley 1972, Ch. 3):

$$K = ku_* y \qquad (30)$$

where k is von Kármán's constant, with a value of 0.4. We use this relationship to enforce internal consistency on the model by equating the average value of K from eq. (30) over the constant-shear layer to the value of K used as a parameter in the model. Hence we require

$$K = ku_* (\tfrac{1}{2}\ 0.4\ell_m) \qquad (31)$$

where, from (29),

$$u_* = (2u_m K/\ell_m)^{1/2} \qquad (32)$$

and so

$$K = \left(2(0.2k)^2\right) u_m \ell_m = \eta u_m \ell_m \qquad (33)$$

where η is 0.0128.

From (25), (26), and (27), we have the relationship between θ_o and u_m as

$$u_m = e^{-\pi/4}\theta_o (C_p/2T_a)^{1/2} \qquad (34)$$

or

$$u_m = 0.585\theta_o, \quad \text{m/s} \qquad (35)$$

for θ_o in °C and T_a = 305°K.

Using (33) in (19) allows us to relate ℓ $(= \frac{4}{\pi}\ell_m)$ and u_m, thus closing the model:

$$\ell_m = \sqrt{2}\, e^{-\pi/4} (\tfrac{\pi}{4})^2 \eta C_p \theta_o / g \sin\alpha \qquad (36)$$

or

$$\ell_m/u_m = 2\eta (\tfrac{\pi}{4})^2 (C_p T_a)^{1/2}/g \sin\alpha. \qquad (37)$$

For an ambient temperature of 305°K (90°F), this ratio becomes simply

$$\ell_m/u_m = 0.892/\sin\alpha \quad \text{(sec)}. \qquad (38)$$

The relationship between u_m and elevation above the valley floor graphed in the text rests on the assumption that the temperature lapse rate of the ambient atmosphere is adiabatic, or about 0.01°C/m, so

$$\theta_o = 5.0 + 0.01z, \quad ^\circ\text{C} \qquad (39)$$

where z is in meters. Equations (35), (38), and (39) represent the core of this model.

The windspeed profile with distance normal to the surface (27) can be written in terms of the distance ℓ_m as

$$u/u_m = \sqrt{2}\ \exp(\pi/4(1 - y/\ell_m))\sin(\frac{\pi}{4}\frac{y}{\ell_m}). \qquad (40)$$

This profile is used in the application of the model to the prediction of surface fire behavior as described in the text (equation 2) and detailed in appendix B.

APPENDIX B: MIDFLAME WINDSPEED VALUES

The "midflame windspeed" input required by the mathematical model (Rothermel 1972) used to predict wildland fire behavior[4] has been interpreted as the mean windspeed of the incident wind field over the vertical extent of the flame (Baughman and Albini 1980). Using this approach, the windspeed profile developed by the theory of appendix A is used to calculate an average windspeed over the "height" range from the top of the fuelbed to the tip of the flame.

The stylized fuel models employed to characterize wildland fuels (Albini 1976) can be described for the present purpose by the fuelbed height, H, and the height of a flame extending above the fuelbed a distance H_F. For each fuel model, a representative flame height was established by using the flame length for that fuel model burning under conditions of no wind, no slope, and typical fuel moisture content. Table 4 summarizes the heights used in this application. Note that while 13 stylized fuel models are described in Albini (1976), only the 10 listed in table 4 are likely to be encountered on open slopes which would experience convective wind.

For the present purpose, the heights listed in table 4 are taken to be the same as the distances measured normal to the slope for the same typical fuel descriptions.

Table 4. Fuelbed heights and flame heights for 10 stylized wildland fuel models that may be encountered on open slopes

Fuel model	Fuelbed height		Typical flame height	
	ft	m	ft	m
1. Short grass	1.0	0.30	1.0	0.30
2. Open timber (grass and understory)	1.0	.30	1.6	.49
3. Tall grass	2.5	.76	2.7	.82
4. Chaparral	6.0	1.83	4.9	1.49
5. Brush	2.0	.61	.92	.28
6. Dormant brush, hardwood slash	2.5	.76	1.4	.43
10. (Used for) overgrown logging slash	1.0	.30	1.6	.49
11. Light logging slash	1.0	.30	1.1	.34
12. Medium logging slash	2.3	.70	2.7	.82
13. Heavy logging slash	3.0	.91	3.7	1.13

[4]See footnote 1.

In the situation that the fire has burned up the slope and consumed the fuel below the present fire position on the slope, the location of the plane $y = 0$ used as a mathematical boundary on which the windspeed vanishes is clearly the surface of the slope. But when a fire *starts* on a slope, the slope surface below the fire location will presumably be covered by vegetation. Here we presume that the fuelbed used to describe the fire behavior extends below the fire when this situation arises. The complication introduced by this surface covering is that the vegetation offers such resistance to fluid motion that the windspeed profile is displaced away from the surface of the slope by an amount nearly equal to the height of the vegetation cover. The exact location of the mathematical boundary surface for the wind field is uncertain in this case. Because we must have a zero-windspeed boundary location to proceed, we simply choose it to be at 77 percent of the height of the fuelbed. The factor 0.77 is not entirely arbitrary. It coincides with the height at which the windspeed would mathematically extrapolate to zero when the windspeed profile over the vegetation is the logarithmic profile typical of constant shear layers under neutral stability (Albini and Baughman 1979).

Using the assumptions outlined above, the midflame windspeed can be written as

$$\bar{u} = \int_{H-\Delta H}^{H_F+H-\Delta H} u(y)\,dy/H_F \qquad (1)$$

where

$u(y)$ is the windspeed at the normal distance y from the zero-velocity surface of the slope
H is the height of the fuelbed
H_F is the height of the flame above the fuelbed
ΔH is the distance from the physical surface of the slope to the zero-velocity surface.

Since

$$u(y) = u_m\sqrt{2}\,\sin(\pi y/4\ell_m)\exp(\tfrac{\pi}{4}(1 - y/\ell_m)) \qquad (2)$$

(appendix A, eq. 40), the integral is readily found, giving

$$\bar{u}/u_m = \frac{2}{\pi}\frac{\ell_m}{H_F}\sqrt{2}((\sin x + \cos x)\exp(\tfrac{\pi}{4} - x))\Big|_b^a \qquad (3)$$

where

$$a = \tfrac{\pi}{4}(H - \Delta H)/\ell_m \qquad (4)$$

$$b = \tfrac{\pi}{4}(H_F + H - \Delta H)/\ell_m. \qquad (5)$$

Whenever the upper limit of the integral in (1) does not exceed the height at which the windspeed is essentially linear with y, the expression for $\bar{u}$ simplifies greatly. Using eq. (28), appendix A

$$u(y) \doteq 2u_m y/\ell_m \qquad (6)$$

gives

$$\bar{u} \doteq (2u_m/\ell_m)(H - \Delta H + H_F/2). \qquad (7)$$

Because of the relationship between u_m and ℓ_m (eq. 38, appendix A), the competing effects of higher windspeed and greater length scale cancel, making $\bar{u}$ a function only of the fuel-bed parameters and the slope angle:

$$\bar{u} \doteq (2/0.892)(H - \Delta H + H_F/2)\sin \alpha \tag{8}$$

where the units of $\bar{u}$ are the length units of $H-\Delta H+H_F/2$ per second. For fuel models 1, 2, 5, 6, and 11, this simple approximation applies reasonably well for all cases. For fuel models 3, 4, 12, and 13, it applies only when

$$H - \Delta H + H_F \leq 0.4\ell_m. \tag{9}$$

For these four models, (8) represents a rough upper bound for the midflame windspeed. The tables given in the text are calculated from (3) for all fuel models, but (8) can be used for quick manual estimation where it applies.

☆U.S. GOVERNMENT PRINTING OFFICE 1982-0-576-026/7

Albini, F. A., D. J. Latham, and R. G. Baughman.
1981. Estimating upslope convective windspeeds for predicting wildland fire behavior. USDA For. Serv. Res. Pap. INT-257, 19 p. Intermt. For. and Range Exp. Stn., Ogden, Utah.

A mathematical model for the near-surface flow of air up a sun-heated slope is derived. The model is used to produce tables and graphs for estimating "midflame" windspeeds as needed for predicting wildland fire behavior. The model applies on open or sparsely-forested slopes when there is otherwise no wind, from midday to late afternoon on clear summer days.

KEYWORDS: convective wind, slope wind, midflame windspeed

Albini, F. A., D. J. Latham, and R. G. Baughman.
1981. Estimating upslope convective windspeeds for predicting wildland fire behavior. USDA For. Serv. Res. Pap. INT-257, 19 p. Intermt. For. and Range Exp. Stn., Ogden, Utah.

A mathematical model for the near-surface flow of air up a sun-heated slope is derived. The model is used to produce tables and graphs for estimating "midflame" windspeeds as needed for predicting wildland fire behavior. The model applies on open or sparsely-forested slopes when there is otherwise no wind, from midday to late afternoon on clear summer days.

KEYWORDS: convective wind, slope wind, midflame windspeed

The Intermountain Station, headquartered in Ogden, Utah, is one of eight regional experiment stations charged with providing scientific knowledge to help resource managers meet human needs and protect forest and range ecosystems.

The Intermountain Station includes the States of Montana, Idaho, Utah, Nevada, and western Wyoming. About 231 million acres, or 85 percent, of the land area in the Station territory are classified as forest and rangeland. These lands include grasslands, deserts, shrublands, alpine areas, and well-stocked forests. They supply fiber for forest industries; minerals for energy and industrial development; and water for domestic and industrial consumption. They also provide recreation opportunities for millions of visitors each year.

Field programs and research work units of the Station are maintained in:

Boise, Idaho

Bozeman, Montana (in cooperation with Montana State University)

Logan, Utah (in cooperation with Utah State University)

Missoula, Montana (in cooperation with the University of Montana)

Moscow, Idaho (in cooperation with the University of Idaho)

Provo, Utah (in cooperation with Brigham Young University)

Reno, Nevada (in cooperation with the University of Nevada)

Estimating upslope convective windspeeds for predicting wildland
Albini, F. A. (Frank A.) cn;Latham, Don J. cn;Baughman, Robert C
CAT92274314
U.S. Department of Agriculture, National Agricultural Library
[56] estimatingupslop257albi
Sep 23, 2013
e s t i m a t i n g u p s l o p 2 5 7 a l b i
S T 0 0 0 3 2 8